

Ozernovskite, $\text{Fe}^{3+}_4(\text{Te}^{4+}\text{O}_4)(\text{Te}^{4+}\text{O}_3)_4(\text{H}_2\text{O})_7$, a new supergene mineral with a unique crystal structure containing two types of tellurite polyhedra

Igor V. Pekov^{1*}, Sergey N. Britvin^{2,3}, Petr A. Pletnev¹, Nikita V. Chukanov⁴, Dmitry I. Belakovskiy⁵, Vasily O. Yapaskurt¹ and Anna G. Turchkova¹

¹Faculty of Geology, Moscow State University, Vorobievsky Gory, 119991 Moscow, Russia

²Saint Petersburg State University, 7/9 Universitetskaya nab., St. Petersburg, 199034 Russia

³Nanomaterials Research Center, Kola Science Center, Russian Academy of Sciences, 184209 Apatity, Murmansk region, Russia

⁴Federal Research Center of Problems of Chemical Physics and Medicinal Chemistry, Russian Academy of Sciences, 142432 Chernogolovka, Moscow region, Russia

⁵Fersman Mineralogical Museum of the Russian Academy of Sciences, Leninsky Prospekt 18-2, 119071 Moscow, Russia

*E-mail: igorpekov@mail.ru

Running title: Ozernovskite, a new mineral

Abstract

The new mineral ozernovskite, ideally $\text{Fe}^{3+}_4(\text{Te}^{4+}\text{O}_4)(\text{Te}^{4+}\text{O}_3)_4(\text{H}_2\text{O})_7$, was found in the oxidation zone of the Ozernovskoe gold deposit, Kamchatka, Russia and named after the locality; IMA-accepted symbol is Ozn. The associated minerals are sonoraite, mandarinoite–telluromandarinoite series members, poughite, emmonsite, tellurite and goethite; the primary minerals in this assemblage are Se-enriched native tellurium, pyrite, maletoyvayamite, tetrahedrite-group minerals of the goldfieldite series, fischesserite, gachingite, bohdanowiczite, paraganajuatite, enargite, quartz, dickite, and baryte. Ozernovskite occurs as long-prismatic to acicular crystals up to $0.03 \times 0.05 \times 1 \text{ mm}^3$ usually assembled in sprays, radial clusters, bush-like aggregates or spherulites up to 2 mm across which sometimes form incrustations up to $1 \times 2.5 \text{ cm}^2$. It is transparent, olive green, yellowish-green or yellow, with vitreous lustre. $D_{\text{calc.}}$ is 3.812 g/cm^3 . Ozernovskite is optically biaxial (–), α 1.915(10), β 1.94(1), γ 1.95(1); pleochroism is weak: Z (pale yellow) > Y (very pale yellow) > X (colourless). The IR spectrum is given. The chemical composition (wt.%, electron microprobe, H_2O by stoichiometry) is Fe_2O_3 25.85, SeO_2 2.69, TeO_2 60.12, As_2O_5 0.57, SO_3 0.08, $\text{H}_2\text{O}_{\text{calc}}$ 10.14, total 99.58. The empirical formula, calculated based on 23 O *apfu*, is $\text{Fe}^{3+}_{3.98}(\text{Te}^{4+}_{4.63}\text{Se}^{4+}_{0.30}\text{As}^{5+}_{0.06}\text{S}^{6+}_{0.01})_{\Sigma 5.00}\text{O}_{16}\cdot 7\text{H}_2\text{O}$. Ozernovskite is monoclinic, *C2/c*, *a* 25.923(3), *b* 10.4192(14), *c* 7.902(1) Å, β 93.415(4)°, *V* 2130.5(5) Å³, and *Z* = 4. The

strongest reflections of the powder XRD pattern [$d, \text{\AA}(I)(hkl)$] are: 12.92(78)(200), 9.67(100)(110), 5.206(24)(020, -311), 3.557(24)(421), 3.481(31)(710), 3.329(26)(312), 3.151(25)(022), 3.007(27)(-331, -602) and 2.885(26)(530, -422). The crystal structure of ozernovskite (solved by SCXRD, $R_1 = 0.0142$) represents a new structure type. It is based upon an open framework composed of dimers of edge-sharing $[\text{Fe}^{3+}\text{O}_5(\text{H}_2\text{O})]$ octahedra, similar dimers of $[\text{Fe}^{3+}\text{O}_6]$ octahedra, trigonal pyramids $[\text{Te}^{4+}\text{O}_3]$ and polyhedra $[\text{Te}^{4+}\text{O}_4]$; weakly bonded H_2O molecules are located in wide intra-framework channels. Ozernovskite is the first natural tellurite which contains both $[\text{TeO}_3]$ and $[\text{TeO}_4]$ anionic units.

Keywords: ozernovskite; new mineral; hydrous iron tellurite; $(\text{TeO}_4)^{4-}$ group; crystal structure; oxidation zone of ore deposit; Ozernovskoe gold deposit; Kamchatka.

Introduction

Tellurium is among the scarcest chemical elements in nature: its average content in the Earth's crust is estimated as 1–5 $\mu\text{g kg}^{-1}$ (Emsley, 2011). Despite of this, more than 210 valid minerals with species-defining Te are known (Pasero, 2025), with some tellurides being significant ore minerals of gold and silver. No doubts that the diversity of Te minerals is mainly caused by the crystal chemical individuality of tellurium which strongly hampers its substitution for other elements, including chemically related sulfur and selenium, especially in oxygen compounds. Oxygen-bearing tellurium minerals preferentially confine to the oxidation zone of telluride ores, where they are comprised mainly by tellurites (TeIV) and tellurates (TeVI). Detailed information on the crystal chemistry of oxygen compounds of tellurium and its behavior in supergene natural systems can be found in two recent comprehensive works (Christy *et al.*, 2016; Missen *et al.*, 2020) and numerous references therein. In the oxysalts, S, Se and Te are known in two valence forms, being hexa- and tetravalent. However, there is a very strong difference between the relative abundance of hexa- and tetravalent forms of S, Se and Te in oxysalt minerals. Sulfates are very abundant in nature whereas sulfites are extremely rare. Opposite behavior is observed for selenium: selenites are common in the oxidation zone of selenide-bearing ores whereas selenate minerals are very rare. Tellurium easily adopts both tetra- and hexavalent states in the oxygen-bearing minerals and, as a result, tellurites and tellurates are distributed in the oxidation zone of ore deposits in comparable amounts. These regularities are connected with the standard enthalpies of formation of the compounds of S, Se and Te in respective oxidation states (Greenwood and Earnshaw, 1997). Natural oxygen compounds of Te^{4+} and Te^{6+} are numerous: *ca.* 105 such valid mineral species are now known (Pasero, 2025) (*i.e.*, about a

half of whole number of Te minerals), that is a record number for such a scarce chemical element.

In this paper, we describe the new tellurite mineral ozernovskite which has a remarkable crystal chemical feature – the presence of both $[\text{Te}^{4+}\text{O}_3]$ and $[\text{Te}^{4+}\text{O}_4]$ anionic groups in the structure. Ozernovskite (Cyrillic: озерновскит) is named after the discovery locality, the Ozernovskoe gold deposit at Kamchatka. Both the new mineral and its name have been approved by the IMA Commission on New Minerals, Nomenclature and Classification (IMA CNMNC), IMA2021–059. The IMA-accepted symbol is Ozn. The type specimen is deposited in the systematic collection of the Fersman Mineralogical Museum, Moscow with the catalogue number 97681.

Occurrence and general appearance

The Ozernovskoe gold deposit is situated in the Pravaya Uka – Levaya Ozernaya interfluve, 115 km North of the town of Klyuchi (700 km North of Petropavlovsk-Kamchatsky), Kamchatka peninsula, Far-Eastern Region, Russia. It is an epithermal deposit of acid-sulfate/high-sulfidation (AS/HS) type which is confined to the Pravaya Uka long-lived volcanotectonic structure. In terms of mineral composition of ores, the Ozernovskoe deposit belongs to the gold-sylvanite-goldfieldite subtype of the telluride type of Au-Ag deposits and is characterized by a general prevailing of gold over silver ([Kudaeva *et al.*, 2024 and references therein](#)). The Ozernovskoe ores are outstandingly diverse in the general mineral composition and, in particular, in mineral forms of gold. This metal is concentrated here in tellurides (sylvanite, krennerite, calaverite), selenotellurides (maletoyvayamite, gachingite), selenides (fischesserite), and in the form of native gold. The gold minerals are associated, in different kinds of ores, with pyrite, Te- and Se-rich members of the tetrahedrite, goldfieldite and *ústalečite* subgroups, Se-bearing native tellurium, hessite, bohdanowiczite, paraganajuatite, skippenite, naumannite, selenodantopaite, bambollaite, clausthalite and some other sulfides, selenides and tellurides. The ore mineralization is concentrated in veins mainly consisting of quartz, typically with subordinate dickite and baryte ([Kovalenker and Plotinskaya, 2005](#); [Spiridonov *et al.*, 2009](#); [Kudaeva *et al.*, 2024](#); [Strelnikov *et al.*, 2025](#); our data).

One of the brightest features of the Ozernovskoe ores is the presence of unusually high-grade native tellurium mineralization. Native tellurium is mainly represented by Se-enriched variety which typically contains from 13 to 30 wt.% Se that corresponds to the range

from (Te_{0.80}Se_{0.20}) to (Te_{0.59}Se_{0.41}) in atomic proportions. This mineral occurs as aggregates of elongate crystals up to 1 cm long which form, together with quartz and dickite, nests and veinlets up to 10 cm thick and, quite often, over 1 m long. Therein, the amount of native tellurium varies from several per cent to 50–60 vol.%. Pyrite, maletoyvayamite, minerals of the goldfieldite subgroup, fischerite, gachingite, bohdanowiczite, paraganajuatite, enargite, and baryte occur in minor amounts (Strelnikov *et al.*, 2025; our new data).

In the upper part of the BAM area of the Ozernovskoe deposit, uncovered by an open pit, the oxidized ores are sporadically distributed. In the zones enriched with native tellurium, a supergene mineralization forms "nests" up to several meters across which typically intimately adjoin with almost unaltered primary ores. Earthy brown goethite (limonite) is the major supergene mineral there. Selenium-bearing native tellurium alters to the association of fine-grained native selenium and different oxygen minerals of Te, some of which contain Se impurity. Sporadically, the secondary Te mineralization is very rich. In this supergene assemblage of Te-Se-O minerals, we have found minerals of the mandarinoite–telluromandarinoite series (Pekov *et al.*, in press), emmonsite, sonoraite, poughite, tamboite, metatamboite, rajite, tlapallite, tellurite, paratellurite, and two new mineral species, rudolfhermannite (Pekov *et al.*, 2022) and ozernovskite.

Ozernovskite originates from the Orebody No. 5 of the BAM area of the Ozernovskoe deposit. The specimens with the new mineral were collected from the operating open pit. The holotype material was found in the beginning of 2020 and additional material was collected in 2020–2022.

Ozernovskite occurs as long-prismatic to acicular crystals up to 0.03 mm × 0.05 mm × 1 mm³. They are elongated along [001] and typically flattened on {010}; split, divergent individuals are common. Polysynthetic contact twins, presumably on {100}, were observed under the microscope in polarized transmitted light. The thinnest individuals are hair- or spear-like. Crystals are usually assembled in sprays, radial clusters, bush-like aggregates, cross- or sun-shaped spherulites and rosettes [Figs. 1(a-c) and 2(a-d)] up to 2 mm across. Crystals and aggregates of ozernovskite are separated from each other or, rarely, form incrustations, solid (up to 5 mm × 5 mm) or interrupted (up to 1 cm × 2.5 cm), which overgrow quartz, dickite or goethite [Figs. 1(a-b)] in cavities and cracks. Other minerals closely associated with ozernovskite are sonoraite [most commonly, Figs. 2(a-c)], mandarinoite–telluromandarinoite series members (Fig. 1b), poughite (Fig. 1c), emmonsite, and tellurite. Oriented, epitactic overgrowing of numerous tiny crystals of emmonsite, usually forming chain-like parallel intergrowths, on ozernovskite crystals (Fig. 3) is common.

All quantitative analytical data given below were obtained from the holotype material.

Physical properties and optical data

Ozernovskite is olive green, yellowish-green, light greenish-yellow or yellow with olive hue; the thinnest acicular or hair-like crystals are pale yellowish to almost colourless. It is transparent, with light yellow streak and vitreous lustre. Ozernovskite is brittle. Cleavage or parting was not observed, the fracture is uneven. The Mohs hardness is *ca.* 3. The density calculated using the empirical formula and unit-cell volume found from the single-crystal X-ray diffraction (SCXRD) data is 3.812 g/cm³.

Ozernovskite is optically biaxial (–), with $\alpha = 1.915(10)$, $\beta = 1.94(1)$, $\gamma = 1.95(1)$ (589 nm; measured in highly refractive immersion liquids); $2V$ was not measured; $2V_{\text{calc.}} = 64^\circ$ (however, this value seems rather formal because refractive indices are measured with significant uncertainties due to high refraction of the mineral). Dispersion of optical axes was not observed. Orientation: $Y = b$. In plane-polarized light ozernovskite is weakly pleochroic, with the following absorption scheme: Z (pale yellow) $>$ Y (very pale yellow) $>$ X (colourless).

Infrared spectroscopy

In order to obtain IR absorption spectra of ozernovskite and, for comparison, of the remotely related (see below) mineral emmonsite $\text{Fe}^{3+}_2(\text{Te}^{4+}\text{O}_3)_3 \cdot 2\text{H}_2\text{O}$, powdered samples were mixed with anhydrous KBr, pelletized, and analyzed using an ALPHA FTIR spectrometer (Bruker Optics) in the range of 360–3800 cm^{–1}, at a resolution of 4 cm^{–1}. 16 scans were collected for each spectrum. The IR spectrum of an analogous pellet of pure KBr was used as a reference.

The assignment of absorption bands in the IR spectrum of ozernovskite (Fig. 4, curve *a*) is as follows:

2400–3400 cm^{–1} – O–H stretching vibrations of H₂O molecules;

1540–1650 cm^{–1} – bending vibrations of H₂O molecules;

630–780 cm^{–1} – Te⁴⁺–O stretching vibrations;

430–520 cm^{–1} – O–Te⁴⁺–O bending and Fe³⁺–O stretching vibrations;

373 cm^{–1} – lattice mode, possibly involving H₂O libration.

Weak absorptions in the range 1000–1450 cm^{–1} correspond to overtones and/or combination modes.

Emmonsite is chemically related to ozernovskite but does not contain Te in four-fold coordination. In the range of vibrations of tellurite groups, the IR spectrum of ozernovskite

differs from that of emmonsite (Fig. 4, curve *b*) by the presence of distinct peaks at 672 and 520 cm^{-1} (in the IR spectrum of emmonsite only a shoulder at 670 cm^{-1} is observed). Based on this fact, one can suppose that the bands at 672 and 520 cm^{-1} may be related to vibrations of the TeO_4^{4-} group. In the range of 2000 – 3700 cm^{-1} , the IR spectrum of ozernovskite differs from that of emmonsite by more intense bands of H_2O and stronger hydrogen bonds.

According to the correlation $\nu (\text{cm}^{-1}) = 3592 - 304 \cdot 10^9 \cdot \exp[-d_{D \cdots A}/0.1321]$ for hydrogen bonds (Libowitzky, 1999), the bands at 3365, 3275, 3140, 2907, and 2420 cm^{-1} correspond to the $D \cdots A$ distances of 2.78, 2.73, 2.685, 2.63, and 2.56 Å which can be put in accordance with the $D \cdots A$ values of 2.787, 2.745, 2.680, 2.644+2.647, and 2.612 Å determined as a result of the crystal structure refinement (see below). A lowered value of the wavenumber of the band at 2420 cm^{-1} as compared to that expected from the correlation suggested by Libowitzky (1999) is due to a large $D\text{--}H \cdots A$ angle which is close to 180°.

Bands of carbonate, borate, or nitrate groups are not observed in the IR spectrum of ozernovskite. The comparison of the IR spectrum of ozernovskite with IR spectra of numerous natural tellurates and tellurites published in the reference books by Chukanov (2014), Chukanov and Chervonnyi (2016), and Chukanov and Vigasina (2020) shows that the IR spectrum of ozernovskite is individual and can be used as a reliable diagnostic tool.

Chemical data

The chemical composition of ozernovskite was studied by electron microprobe using a Jeol JSM-6480LV scanning electron microscope equipped with an INCA-Wave 500 wavelength-dispersive spectrometer (WDS) in the Laboratory of Analytical Techniques of High Spatial Resolution, Dept. of Petrology, Lomonosov Moscow State University. The operating conditions were: an acceleration voltage 20 kV and a beam current 10 nA; the electron beam was rastered to the 5 $\mu\text{m} \times 5 \mu\text{m}$ area. Chemical data (in wt.%, averaged for five spot analyses obtained from five crystals extracted from the holotype specimen) are given in Table 1. H_2O was not analysed because of paucity of pure material. The content of H_2O was calculated by stoichiometry (Table 1) based on the crystal structure data (see below). The presence of H_2O molecules is also confirmed by the IR spectrum (Fig. 4). Contents of other elements with atomic numbers higher than that of carbon are below detection limits.

The empirical chemical formula of ozernovskite calculated on the basis of 23 O atoms (including 7 O atoms belonging to H_2O molecules) per formula unit is $\text{Fe}^{3+}_{3.98}(\text{Te}^{4+}_{4.63}\text{Se}^{4+}_{0.30}\text{As}^{5+}_{0.06}\text{S}^{6+}_{0.01})_{\Sigma 5.00}\text{O}_{16} \cdot 7\text{H}_2\text{O}$. The idealised formula is $\text{Fe}^{3+}_4\text{Te}^{4+}_5\text{O}_{16} \cdot 7\text{H}_2\text{O}$ or, in accordance with the crystal structure data,

$\text{Fe}^{3+}_4(\text{Te}^{4+}\text{O}_4)(\text{Te}^{4+}\text{O}_3)_4(\text{H}_2\text{O})_7$ which requires Fe_2O_3 25.68, TeO_2 64.18, H_2O 10.14, total 100 wt%.

The Gladstone-Dale compatibility index $1 - (K_p/K_c)$ (Mandarino, 1981) is equal to -0.003 (rated as superior).

X-ray crystallography and crystal structure determination

The powder XRD data for ozernovskite (Table 2) were collected in Debye-Scherrer geometry by means of a Rigaku R-Axis Rapid II diffractometer equipped with curved (semi-cylindrical) imaging plate detector ($r = 127.4$ mm), using $\text{CoK}\alpha$ radiation ($\lambda = 1.79021$ Å) generated by a rotating anode (40 kV, 15 μA) with microfocus optics; exposure time was 15 min. The imaging plate was calibrated against a NIST Si standard. The image-to-profile data processing was performed using *osc2xrd* software (Britvin *et al.*, 2017). Parameters of the monoclinic unit cell of ozernovskite refined from the powder data using the program package STOE WinXPOW, version 2.22 are: $a = 25.936(8)$, $b = 10.433(3)$, $c = 7.900(2)$ Å, $\beta = 93.42(3)^\circ$, and $V = 2134(2)$ Å³.

SCXRD study of ozernovskite was carried out at room temperature on a crystal of $0.02 \times 0.03 \times 0.08$ mm³ in size using a Bruker Kappa APEX DUO diffractometer equipped with a microfocus X-ray tube and Photon III hybrid photon counting detector. Data collection and reduction procedures were carried out using Bruker APEX3 software. The crystal structure was solved by direct methods and refined to $R_1 = 0.0142$ using *SHELX-2014* set of programs (Sheldrick, 2015) incorporated into the Olex2 v.1.5 graphical user environment (Dolomanov *et al.*, 2009). Crystal parameters, data collection information and structure refinement details are presented in Table 3, coordinates and isotropic displacement parameters of atoms and site occupancies are given in Table 4, anisotropic displacement parameters in Table 5, selected interatomic distances and bond-valence sums in Table 6, and hydrogen bond geometry in Table 7.

Discussion

Ozernovskite has a unique crystal structure. It is based upon an open framework composed of dimers of edge-sharing $[\text{Fe}^{3+}\text{O}_5(\text{H}_2\text{O})]$ octahedra centered by Fe1 cations, similar dimers of $[\text{Fe}^{3+}\text{O}_6]$ octahedra centered by Fe2, trigonal pyramids $[\text{Te}^{4+}\text{O}_3]$ (with Te1 and Te3) and polyhedra $[\text{Te}^{4+}\text{O}_4]$ with Te2) (Tables 4 and 6, Fig. 5). This kind of polyhedron can be described as trigonal bipyramid -1 ligand (Christy *et al.*, 2016). The Te3 site has substitution

of Te by lighter Se. During the structure refinement, the Te3 site was assumed as (Te,Se) and the refined Te:Se ratio (Table 4) is in a good agreement with the electron microprobe data (Table 1). Unlike the H₂O molecule marked as W1 in Tables 4–6, which participates in coordination of Fe1, the weakly bonded H₂O molecules (W2–4 in Tables 4 and 5) are located in wide (*ca.* 7 Å × 9 Å) intra-framework channels running along *c*; these water molecules are omitted in Fig. 5 for clarity.

While the trigonal pyramidal group [Te⁴⁺O₃] is a very common type of anion in oxycompounds of tetravalent tellurium, including minerals, the trigonal bipyramid -1 ligand [Te⁴⁺O₄] is extremely rare, and was unknown among the minerals (Christy *et al.*, 2016). It can be represented as a very distorted variant of square pyramid [Te⁴⁺O₄] known in nabokoite KCu₇(Te⁴⁺O₄)(SO₄)₅Cl (Pertlik and Zemann, 1988). To the best of our knowledge, ozernovskite demonstrates a first example of tellurite which contains both [TeO₃] and [TeO₄] units in the structure.

Trivalent state of iron and tetravalent state of tellurium are clearly confirmed by crystal structure data, including Fe–O and Te–O distances and bond-valence sums (Table 6). The presence of admixed selenium substituting tellurium in the Te3 site with trigonal pyramidal coordination corroborates with tetravalent state of Se. The results of bond-valence calculations (Table 6) also confirm that valence states of Fe³⁺, Te⁴⁺ and Se⁴⁺ are correct.

Epitaxy of emmonsite on ozernovskite (Fig. 3) is probably caused by very close values of the *a* unit-cell parameter of the former (7.90 Å: Pertlik, 1972) and the *c* parameter of the latter (7.902 Å: Table 3). This coincidence, in due course, is caused by similar structural motifs of both minerals along [001] (ozernovskite) and [100] (emmonsite): the dimers of Fe³⁺-centered octahedra connected *via* corner-sharing [TeO₃] groups.

The oxidation zone of the Ozernovskoe deposit is, in particular, interesting as a very bright locality of Fe³⁺ tellurites. They demonstrate here an outstanding diversity and abundance: in some areas, these minerals compose several vol. % of the oxidized gold ore (Pekov *et al.*, in press). In the supergene mineral-forming system at the Ozernovskoe deposit, tellurium is geochemically closely connected mainly to trivalent iron: the Fe³⁺ tellurites act, along with two polymorphs of TeO₂, tellurite and paratellurite, as major carriers of Te here, whereas the role of other secondary tellurium minerals is negligible, including copper tellurites and tellurates – the most typical, often main supergene minerals of Te at many other localities. At Ozernovskoe emmonsite Fe³⁺₂(TeO₃)₃·2H₂O, poughite Fe³⁺₂(TeO₃)₂(SO₄)·3H₂O, sonoraite Fe³⁺TeO₃(OH)·H₂O, and telluromandarinoite Fe³⁺₂[(Te,Se)O₃]₂·5–6H₂O are common minerals and ozernovskite

$\text{Fe}^{3+}_4(\text{Te}^{4+}\text{O}_4)(\text{Te}^{4+}\text{O}_3)_4 \cdot 7\text{H}_2\text{O}$, rudofermannite $\text{Fe}^{3+}_2(\text{TeO}_3)_3 \cdot \text{H}_2\text{O}$, tamboite
 $\text{Fe}^{3+}_3(\text{OH})(\text{SO}_4)(\text{Te}^{4+}\text{O}_3)_3[\text{Te}^{4+}\text{O}(\text{OH})_2](\text{H}_2\text{O})_5$, and metatamboite
 $\text{Fe}^{3+}_3(\text{OH})(\text{SO}_4)(\text{Te}^{4+}\text{O}_3)_3[\text{Te}^{4+}\text{O}(\text{OH})_2](\text{H}_2\text{O})_3$ occur in subordinate amounts. In several specimens we found Cu-Te oxysalts, rajite $\text{CuTe}^{4+}_2\text{O}_5$ and tlapallite $\text{Ca}_4\text{Cu}_6[\text{Te}^{4+}_3\text{Te}^{6+}\text{O}_{12}]_2(\text{Te}^{4+}\text{O}_3)_2(\text{SO}_4)_2 \cdot 3\text{H}_2\text{O}$. In our opinion, these chemical features of the supergene tellurium mineralization at Ozernovskoe is caused by the fact that the two main primary ore minerals here are native tellurium and pyrite, while the role of Cu sulfides (sulfosalts) and other chalcogenides is minor. The presence of tellurites – minerals with tetravalent Te, but not tellurates – minerals with hexavalent Te – at the Ozernovskoe deposit is apparently due to the “immaturity” of the oxidation zone: relict primary ore minerals – native tellurium and pyrite – closely coexist here with supergene Te oxysalts and oxides.

In different specimens ozernovskite is intimately associated with several other Fe^{3+} tellurites: telluromandarinoite (Fig. 1b), poughite (Fig. 1c), sonoraite (Figs. 2a-b), and emmonsite (Fig. 3). As our observations show, there is no regular pattern in the crystallization sequence of these Fe^{3+} tellurites. The intergrowths of ozernovskite with other minerals also have an irregular character, except for the epitaxy of emmonsite on ozernovskite (Fig. 3), which is observed in many specimens. It is caused by some common structure features of these two minerals (see above) whereas from other tellurites ozernovskite strongly differs in terms of crystal structure.

Acknowledgements

We are grateful to the heads and geologists of the SIGMA Company, who supported our works at the Ozernovskoe deposit, and Maria D. Milshina who made colour photographs of the specimens with ozernovskite. We thank three anonymous reviewers and Associate Editor Owen Missen for valuable comments. The mineralogical and crystal chemical studies of ozernovskite were supported by the Russian Science Foundation, grant no. 25-17-00005. The XRD investigation was carried out at the Center for X-Ray Diffraction Research of the Science Park of St. Petersburg State University within the framework of project 125021702335-5. The IR spectroscopy study was performed in accordance with the state task, registration number 124013100858-3.

References

- Breese N.E. and O'Keeffe M. (1991). Bond-Valence parameters for solids. *Acta Crystallographica*, **B47**, 192–197.
- Britvin S.N., Dolivo-Dobrovolsky D.V. and Krzhizhanovskaya M.G. (2017) Software for processing the X-ray powder diffraction data obtained from the curved image plate detector of Rigaku RAXIS Rapid II diffractometer. *Zapiski Rossiiskogo Mineralogicheskogo Obshchestva*, **146**, 104–107 (in Russian).
- Christy A.G., Mills S.J and Kampf A.R. (2016) A review of the structure architecture of tellurium oxycompounds. *Mineralogical Magazine*, **80**, 415–545.
- Chukanov N.V. (2014) *Infrared Spectra of Mineral Species: Extended Library*. Springer, Dordrecht, 1716 pp.
- Chukanov N.V. and Chervonnyi A.D. (2016) *Infrared Spectroscopy of Minerals and Related Compounds*. Springer, Cham, 1109 pp.
- Chukanov N.V. and Viggasina M.F. (2020) *Vibrational (Infrared and Raman) Spectra of Minerals and Related Compounds*. Springer, Dordrecht, 1376 pp.
- Dolomanov O.V., Bourhis L.J., Gildea R.J., Howard J.A. and Puschmann H. (2009) OLEX2: a complete structure solution, refinement and analysis program. *Journal of Applied Crystallography*, **42**, 339–341.
- Emsley J. (2011) *Nature's Building Blocks: An A-Z Guide to the Elements*. Oxford University Press, Oxford.
- Greenwood N.N. and Earnshaw A. (1997) *Chemistry of the Elements*. 2nd edition. Reed Educational and Professional Publishing Ltd, Oxford.
- Kovalenker V.A. and Plotinskaya O.Yu. (2005) Te and Se mineralogy of Ozernovskoe and Prasolovskoe epithermal gold deposits, Kuril – Kamchatka volcanic belt. *Geochemistry, Mineralogy and Petrology*, **43**, 14–19.
- Kudaeva Sh.S., Kozlov V.V., Skilskaya E.D., Sergeeva A.V., Tolstykh N.D. and Shkilev I.A. (2024) New type of gold-bearing mineralization at the Ozernovskoe Au–Te–Se epithermal deposit (Central Kamchatka, Russia). *Geology of Ore Deposits*, **66(5)**, 547–569.
- Libowitzky E. (1999) Correlation of O–H stretching frequencies and O–H···O hydrogen bond lengths in minerals. *Monatshefte für Chemie*, **130**, 1047–1059.
- Mandarino J.A. (1981) The Gladstone-Dale relationship. Part IV. The compatibility concept and its application. *Canadian Mineralogist*, **14**, 498–502.
- Mills S.J. and Christy A.G. (2013) Revised values of the bond-valence parameters for Te^{IV}–O, Te^{VI}–O and Te^{IV}–Cl. *Acta Crystallographica*, **B69**, 145–149.

- Missen O.P., Ram R., Mills S.J., Etschmann B., Reith F., Shuster J., Smith D.J., Brugger J. (2020) Love is in the Earth: A review of tellurium (bio)geochemistry in surface environments. *Earth-Science Reviews*, paper 103150.
- Pasero M. (2025) The New IMA List of Minerals. Available online via: <http://cnmnc.units.it> (November 2025).
- Pekov I.V., Britvin S.N., Pletnev P.A., Yapaskurt V.O., Belakovskiy D.I., Chukanov N.V., Viggasina M.F. and Ponomarev A.P. (2022) Rudolfhermannite, IMA 2021-099. CNMNC Newsletter 66. *Mineralogical Magazine*, **86**, 359–362.
- Pekov I.V., Strel'nikov M.V., Zubkova N.V., Khanin D.A., Yapaskurt V.O., Viggasina M.F., Pletnev P.A., Britvin S.N., Yanson S.Yu. and Pushcharovskiy D.Yu. First natural example of wide isomorphism between selenites and tellurites: A mandarinoite–telluromandarinoite continuous solid-solution series, its crystal chemical and genetic features. *Zapiski Rossiiskogo Mineralogicheskogo Obshchestva*, in press.
- Pertlik F. (1972) Der Strukturtyp von Emmonsit, $\{\text{Fe}_2[\text{TeO}_3]_3 \cdot \text{H}_2\text{O}\} \cdot x\text{H}_2\text{O}$ ($x = 0-1$). *Tschermaks Mineralogische und Petrographische Mitteilungen*, **18**, 157–168.
- Pertlik F. and Zemann J. (1988) The crystal structure of nabokoite, $\text{Cu}_7\text{TeO}_4(\text{SO}_4)_5 \cdot \text{KCl}$: the first example of a Te(IV)O_4 pyramid with exactly tetragonal symmetry. *Mineralogy and Petrology*, **38**, 291–298.
- Sheldrick G.M. (2015) Crystal structure refinement with *SHELXL*. *Acta Crystallographica*, **C71**, 3–8.
- Spiridonov E.M., Filimonov S.V. and Bryzgalov I.A. (2009) A solid solution of fischesserite–naumannite in ores of the Ozernovskoye volcanogenic gold deposit, Kamchatka. *Doklady Rossiiskoy Akademii Nauk*, **425(3)**, 391–394 (in Russian).
- Strel'nikov M.V., Pekov I.V., Yapaskurt V.O., Ksenofontov D.A. and Pletnev P.A. (2025) Selenium-rich native tellurium from Ozernovskoe gold deposit (Kamchatka, Russia) and isomorphism in Te–Se system. *Zapiski Rossiiskogo Mineralogicheskogo Obshchestva*, **154(2)**, 88–105 (in Russian).
- Westrip S.P. (2010) publCIF: software for editing, validating and formatting crystallographic information files. *Journal of Applied Crystallography*, **43**, 920–925.

Table 1. Chemical composition (in wt.%) of ozernovskite.

Constituent	Mean	Range	Standard deviation	Reference material
Fe ₂ O ₃	25.85	25.70 – 26.05	0.15	Fe
SeO ₂	2.69	2.25 – 3.03	0.38	Se
TeO ₂	60.12	58.40 – 62.67	1.70	PbTe
As ₂ O ₅	0.57	0.18 – 0.79	0.23	InAs
SO ₃	0.08	0.07 – 0.08	0.01	FeS ₂
H ₂ O _{calc.} *	10.27			
Total	99.58			

*The content of H₂O is calculated by stoichiometry, for 7 H₂O molecules per formula unit, in accordance with the crystal structure data.

Prepublished article

Table 2. Powder X-ray diffraction data (d in Å) of ozernovskite.

I_{obs}	d_{obs}	I_{calc}^*	d_{calc}^{**}	hkl		I_{obs}	d_{obs}	I_{calc}^*	d_{calc}^{**}	hkl
78	12.92	71	12.938	200		9	2.604	5	2.604	-132
100	9.67	100	9.665	110				3	2.600	-622
6	6.66	1	6.644	310		4	2.527	2	2.523	-332
19	6.46	16	6.469	400		6	2.478	1	2.484	-313
5	6.05	1	6.046	111				3	2.473	041
24	5.206	6	5.210	020				2	2.468	332
		12	5.200	-311		5	2.440	4	2.439	-731
21	4.973	17	4.971	311		5	2.414	4	2.416	440
9	4.838	2	4.833	220		3	2.383	2	2.382	731
10	4.634	5	4.635	510		3	2.336	1	2.341	-513
4	4.354	3	4.347	021				2	2.332	-912
8	4.162	5	4.162	-221		8	2.290	1	2.292	532
11	4.087	3	4.093	-511				7	2.288	223
		7	4.080	221		7	2.254	5	2.256	-10.2.1
6	3.951	2	3.944	002		8	2.215	6	2.215	930
4	3.907	1	3.906	511		4	2.175	2	2.174	042
5	3.843	1	3.837	-202				1	2.171	-732
15	3.666	11	3.664	-421		8	2.131	7	2.129	641
8	3.629	1	3.624	112		3	2.107	1	2.107	10.0.2
24	3.557	18	3.555	421		4	2.097	2	2.098	-133
31	3.481	21	3.484	710				1	2.092	732
26	3.329	25	3.325	312		7	2.030	2	2.035	-11.1.2
5	3.282	1	3.282	402				1	2.029	840
5	3.226	1	3.235	800				5	2.026	350
		2	3.222	330		3	2.012	1	2.011	-151
17	3.170	15	3.164	-131		6	1.993	3	1.992	12.2.0
25	3.151	16	3.144	022		6	1.986	4	1.983	-841
8	3.092	1	3.089	-222		7	1.973	4	1.972	-932
		2	3.086	-512				2	1.970	-351
27	3.007	4	3.013	621		11	1.943	2	1.941	-12.0.2
		15	3.006	-331				10	1.941	-114
		10	3.001	-602		4	1.922	1	1.924	-13.1.1
15	2.929	13	2.928	512				1	1.924	114
26	2.885	10	2.884	530				1	1.918	-404
		14	2.882	-422		4	1.851	-514		
7	2.830	4	2.828	602		9	1.849	2	1.848	14.0.0
17	2.772	5	2.777	422				4	1.846	12.0.2
		14	2.772	910		5	1.792	3	1.794	-13.1.2
11	2.752	7	2.748	820		5	1.780	4	1.777	842
9	2.663	7	2.663	-911						

Table 2 (continue)

I_{obs}	d_{obs}	I_{calc}^*	d_{calc}^*	hkl		I_{obs}	d_{obs}	I_{calc}^*	d_{calc}^*	hkl
4	1.755	1	1.760	443		3	1.591	3	1.589	062
		1	1.759	-714		5	1.573	1	1.574	-553
		2	1.754	604				2	1.573	262
4	1.731	2	1.731	-624		4	1.544	4	1.571	-952
		1	1.730	-804				1	1.545	-444
2	1.707	1	1.706	-13.3.1				1	1.545	16.2.0
		1	1.705	134		2	1.543	-10.2.4		
3	1.697	1	1.696	061		4	1.532	1	1.542	-11.5.1
		1	1.694	10.2.3				2	1.532	-16.2.1
2	1.679	1	1.677	460		3	1.532	952		
4	1.669	4	1.669	13.3.1		3	1.518	2	1.519	315
4	1.658	1	1.661	12.4.0				1	1.518	-515
		2	1.657	933				2	1.515	-753
4	1.640	1	1.641	804		3	1.507	2	1.508	-934
		1	1.641	-12.4.1				1	1.506	17.1.0
2	1.628	1	1.628	-14.2.2		3	1.502	2	1.501	15.3.1
		1	1.626	153		1	1.500	-644		
2	1.616	1	1.616	-353		4	1.498	1	1.500	16.2.1
		1	1.616	-10.0.4				1	1.496	-17.1.1
3	1.606	1	1.611	12.4.1		2	1.480	3	1.479	-13.3.3
		1	1.603	-11.3.3		2	1.462	2	1.459	171
		1	1.603	534		3	1.441	1	1.442	10.6.0

* For the calculated pattern only reflections with intensities ≥ 1 are given; ** for the unit-cell parameters obtained from single-crystal data. The strongest reflections are marked in boldtype.

Table 3. Crystal parameters, data collection and structure refinement details for ozernovskite.

Crystal Data	
Formula	$\text{Fe}^{3+}_4[\text{Te}^{4+}\text{O}_4][\text{Te}^{4+}\text{O}_3][(\text{Te}^{4+}_{0.88}\text{Se}^{4+}_{0.12})\text{O}_3]_3 \cdot 7\text{H}_2\text{O}$
Crystal size (mm^3)	$0.02 \times 0.03 \times 0.08$
Crystal system, space group	Monoclinic, $C2/c$
a, b, c (\AA)	25.923(3), 10.4192(14), 7.902(1)
β ($^\circ$)	93.415(4)
V (\AA^3)	2130.5(5)
Z	4
Data collection and refinement	
Radiation	$\text{MoK}\alpha$ ($\lambda = 0.71073 \text{ \AA}$)
Temperature (K)	296(2)
2θ range ($^\circ$)	4.214 – 51.99
No. of meas., independ. and obs. [$I > 2\sigma(I)$] reflections	23680, 2578, 2473
h, k, l range	$-34 \rightarrow 30, -13 \rightarrow 13, -10 \rightarrow 10$
$F(000)$	2231
μ (mm^{-1})	9.57
Absorption correction	multi-scan
No. refined parameters	159
$R_{\text{int}}, R_{\sigma}$	0.0328, 0.0170
R_1 [$F \geq 4\sigma(F)$], wR_2	0.0157, 0.0342
GoF	1.077
Data completeness	1.000
Residual density (e \AA^{-3}) (min, max)	-0.67, 1.64

Weighting scheme: $w=1/[\sigma^2(F_o^2)+(0.0110P)^2+10.0751P]$ where $P=(F_o^2 + 2F_c^2)/3$

Table 4. Fractional atomic coordinates, isotropic or equivalent isotropic displacement parameters (\AA^2) and site occupancies for ozernovskite^a.

Site ^b	<i>x/a</i>	<i>y/b</i>	<i>z/c</i>	<i>U</i> _{iso/eq}	Occupancy
Fe1 (8 <i>f</i>)	0.71385(2)	0.03066(2)	0.95448(2)	0.00876(5)	Fe
Fe2 (4 <i>e</i>)	1/2	0.68211(2)	3/4	0.01051(6)	Fe
Te1 (8 <i>f</i>)	0.65595(2)	0.40793(2)	0.78368(2)	0.01081(6)	Te
Te2 (8 <i>f</i>)	0.76200(2)	0.24378(4)	0.70372(4)	0.00833(8)	Te
Te3 (8 <i>f</i>)	0.55919(2)	0.50783(4)	0.50350(5)	0.01011(8)	Te _{0.884(3)} Se _{0.116(3)}
O1 (8 <i>f</i>)	0.74922(7)	−0.12629(18)	1.0022(2)	0.0110(4)	O
O2 (8 <i>f</i>)	0.49764(7)	0.62735(18)	0.5013(2)	0.0118(4)	O
O3 (8 <i>f</i>)	0.68788(7)	0.24930(19)	0.7569(2)	0.0138(4)	O
O4 (8 <i>f</i>)	0.72168(8)	0.09152(18)	1.1792(2)	0.0128(4)	O
O5 (8 <i>f</i>)	0.77201(7)	0.11545(18)	0.8824(2)	0.0111(4)	O
O6 (8 <i>f</i>)	0.60379(8)	0.35445(19)	0.9175(3)	0.0155(4)	O
O7 (8 <i>f</i>)	0.61844(8)	0.3979(2)	0.5743(2)	0.0164(4)	O
O8 (8 <i>f</i>)	0.44296(7)	0.56371(19)	0.7445(2)	0.0123(4)	O
OW1 (8 <i>f</i>)	0.83836(8)	0.2417(2)	0.6587(3)	0.0191(4)	O (H ₂ O)
HW1A (8 <i>f</i>)	0.863210	0.276143	0.732601	0.029 ^c	H (H ₂ O)
HW1B (8 <i>f</i>)	0.850453	0.198322	0.589899	0.029 ^c	H (H ₂ O)
OW2 (8 <i>f</i>)	0.91089(10)	0.3376(3)	0.8651(3)	0.0316(6)	O (H ₂ O)
HW2A (8 <i>f</i>)	0.902081	0.413766	0.888521	0.047 ^c	H (H ₂ O)
HW2B (8 <i>f</i>)	0.904048	0.309655	0.970748	0.047 ^c	H (H ₂ O)
OW3 (4 <i>e</i>)	1/2	0.8097(4)	1/4	0.0390(9)	O (H ₂ O)
HW3 (8 <i>f</i>)	0.494499	0.755530	0.154281	0.058 ^c	H (H ₂ O)
OW4 (8 <i>f</i>)	0.5917(2)	0.0914(4)	0.6369(10)	0.1079(19)	O (H ₂ O)
HW4A (8 <i>f</i>)	0.562198	0.123227	0.653173	0.162 ^c	H (H ₂ O)
HW4B (8 <i>f</i>)	0.612398	0.154396	0.647865	0.162 ^c	H (H ₂ O)

^a Crystallographic tables were created using PubCIF software (Westrip, 2010). ^b Site multiplicities and Wyckoff letters are given in parentheses. ^c Hydrogen atoms were located by electron difference mapping and refined using riding model.

Table 5. Anisotropic displacement parameters (\AA^2) for ozernovskite.

Site	U^{11}	U^{22}	U^{33}	U^{12}	U^{13}	U^{23}
Fe1	0.01086(8)	0.00795(8)	0.00757(8)	0.00030(6)	0.00130(6)	-0.00028(6)
Fe2	0.01023(11)	0.01060(12)	0.01088(11)	0.000	0.00203(8)	0.000
Te1	0.01037(9)	0.01161(10)	0.01069(10)	0.00199(6)	0.00241(6)	0.00051(6)
Te2	0.01037(9)	0.01161(10)	0.01069(10)	0.00199(6)	0.00241(6)	0.00051(6)
Te3	0.01103(17)	0.00704(17)	0.00705(16)	0.00028(13)	0.00171(13)	0.00012(13)
O1	0.00779(17)	0.01360(19)	0.00909(17)	0.00044(14)	0.00172(13)	0.00075(14)
O2	0.0183(9)	0.0065(8)	0.0082(8)	0.0024(7)	0.0004(7)	0.0003(7)
O3	0.0102(8)	0.0139(9)	0.0115(9)	0.0006(7)	0.0019(7)	-0.0008(7)
O4	0.0143(9)	0.0120(9)	0.0153(9)	0.0022(7)	0.0031(7)	-0.0001(7)
O5	0.0210(10)	0.0093(9)	0.0082(8)	-0.0015(7)	0.0020(7)	-0.0024(7)
O6	0.0125(9)	0.0110(9)	0.0100(9)	0.0002(7)	0.0015(7)	0.0029(7)
O7	0.0153(9)	0.0149(10)	0.0169(10)	0.0034(8)	0.0067(8)	0.0030(8)
O8	0.0144(9)	0.0249(11)	0.0097(9)	0.0093(8)	-0.0015(7)	-0.0022(8)
OW1	0.0104(9)	0.0157(10)	0.0110(9)	-0.0036(7)	0.0023(7)	0.0005(7)
OW2	0.0128(9)	0.0265(12)	0.0184(10)	-0.0001(8)	0.0046(8)	-0.0114(9)
OW3	0.0375(14)	0.0280(13)	0.0285(13)	-0.0049(11)	-0.0041(11)	0.0028(10)
OW4	0.069(3)	0.0221(19)	0.0248(18)	0.000	-0.0056(18)	0.000

Table 6. Selected interatomic bond lengths (Å) and bond-valence sums (*BVS*, *v.u.*) for cationic sites in ozernovskite.

Bond	Length	Polyhedron	Bond	Length	Polyhedron
Fe1–O1	2.123(2)	Octahedron	Te1–O1	1.902(2)	Trigonal pyramid
Fe1–O1	2.020(2)	[FeO ₅ (H ₂ O)]	Te1–O4	1.885(2)	[:TeO ₃]*
Fe1–O3	1.992(2)		Te1–O5	1.866(2)	
Fe1–O4	1.983(2)		<Te1–O>	1.884	
Fe1–O5	1.951(2)		<i>BVS</i> (Te1)	3.86	
Fe1–OW1	2.032(2)		Te2–O2	2.044(2) × 2	Trigonal bipyramid
<Fe1–O>	2.017		Te2–O8	1.924(2) × 2	-1 ligand [:TeO ₄]*
<i>BVS</i> (Fe1)	3.02		<Te2–O>	1.984	
Fe2–O2	2.037(2)	Octahedron	<i>BVS</i> (Te2)	3.98	
Fe2–O2	2.023(2)	[FeO ₆]	Te3–O3	1.866(2)	Trigonal pyramid
Fe2–O6	1.988(2)		Te3–O6	1.851(2)	[:TeO ₃]*
Fe2–O7	1.970(2)		Te3–O7	1.871(2)	
Fe2–O8	2.078(2)		<Te3–O>	1.863	
Fe2–O8	2.095(2)		<i>BVS</i> (Te3)	3.88	
<Fe2–O>	2.032				
<i>BVS</i> (Fe2)	2.89				

*The symbol ":" means lone electron pair belonging to Te⁴⁺. Bond-valence parameters for Fe are taken from Brese and O'Keeffe (1991), for Te from Mills and Christy (2013).

Table 7. Hydrogen bond geometry (Å, °) for ozernovskite.

<i>D–H···A</i>	<i>D–H</i>	<i>H···A</i>	<i>D···A</i>	<i>D–H···A</i>
OW1–HW1A···OW2	0.92	1.70	2.613 (3)	178
OW1–HW1B···O7 ⁱ	0.79	1.86	2.647 (3)	177
OW2–HW2A···OW4 ⁱⁱ	0.85	1.87	2.645 (5)	151
OW2–HW2B···O6 ⁱⁱⁱ	0.91	1.94	2.679 (3)	137
OW3–HW3···O2 ^{iv}	0.95	1.83	2.751 (3)	162
OW4–HW4A···OW3 ^v	0.85	1.95	2.786 (5)	166

Symmetry codes: (i) $-x+3/2, -y+1/2, -z+1$; (ii) $-x+3/2, y+1/2, -z+3/2$; (iii) $-x+3/2, -y+1/2, -z+2$; (iv) $-x+1, y, -z+1/2$; (v) $-x+1, -y+1, -z+1$

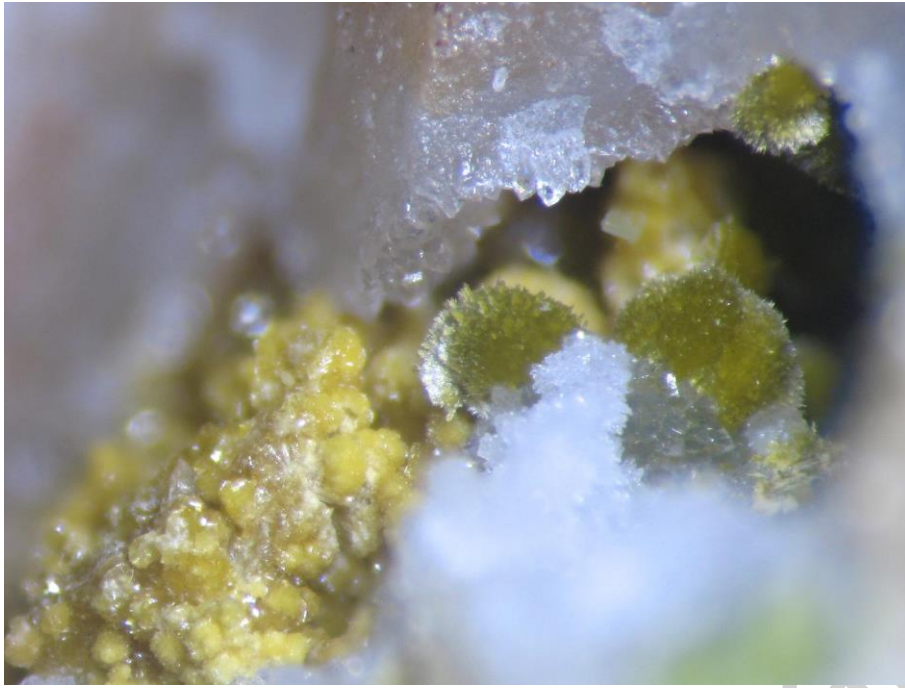


a



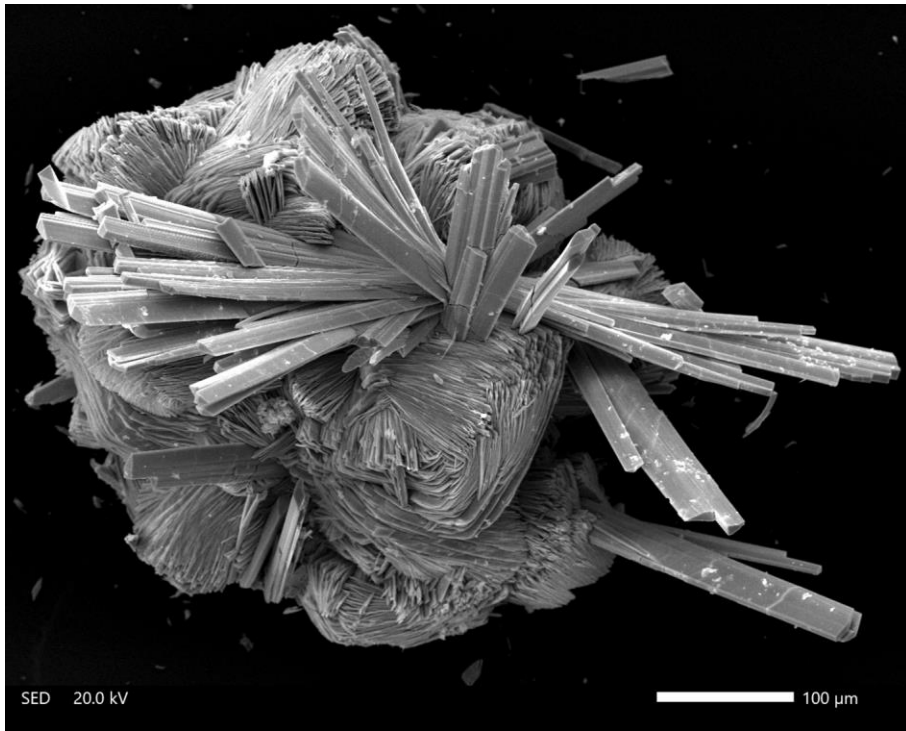
b

Article

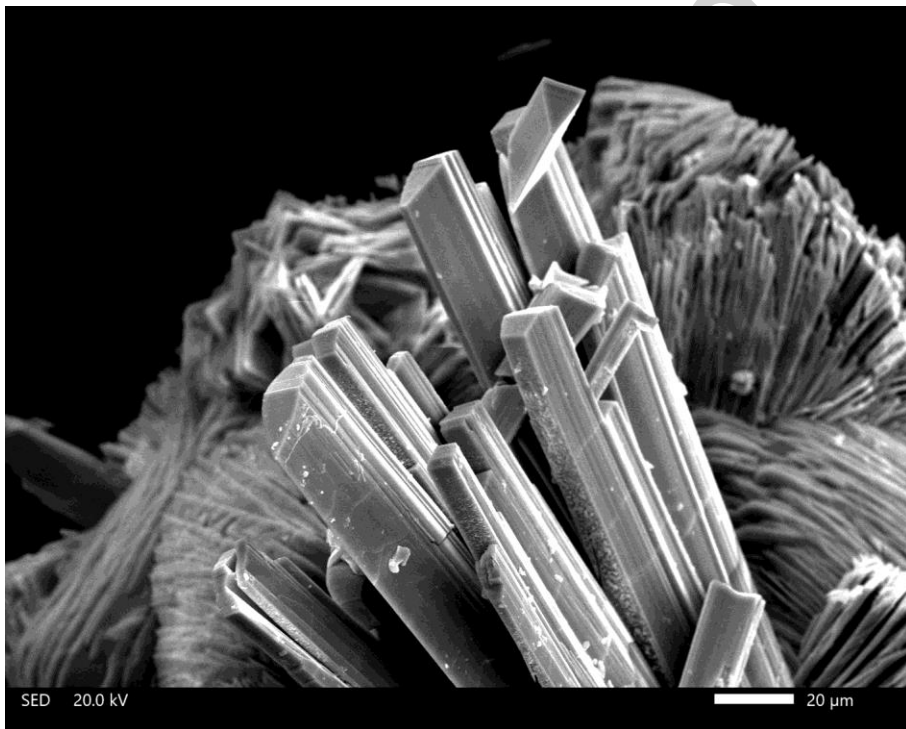


c

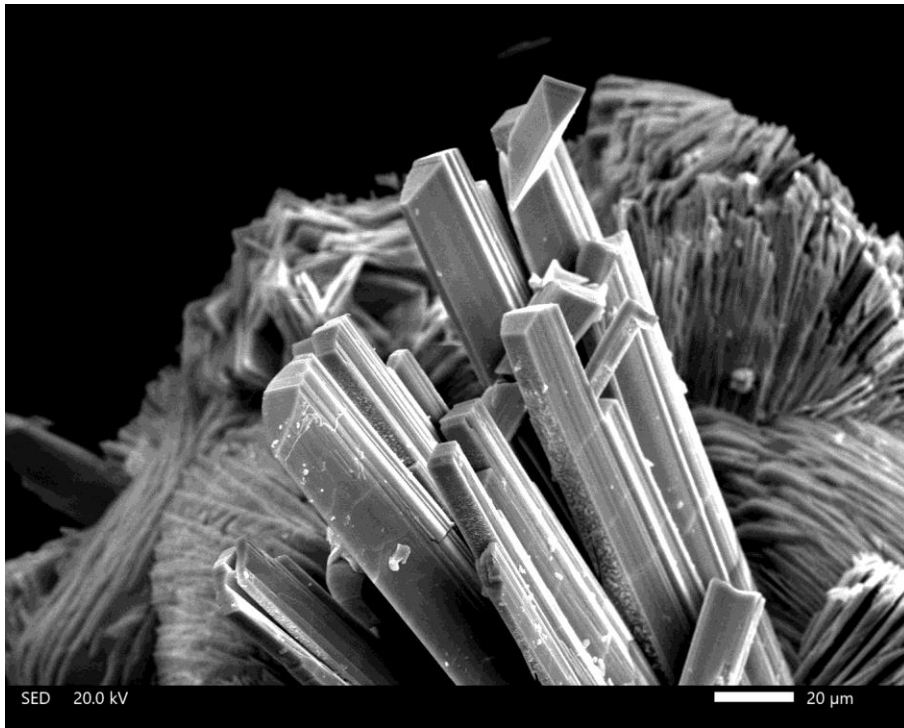
Figure 1. Ozernovskite: (a) clusters of long-prismatic to acicular yellow crystals on colourless quartz partially covered by thin brown goethite film; (b) cross-like cluster of two long-prismatic divergent crystals associated with pale apple-green telluromandarinoite crystals on quartz; (c) olive-green dense radial spherulites with yellow poughite in cavity in veiny quartz. FOV width: a – 2.1 mm, b – 1.1 mm, c – 3.6 mm. Photographed by: a, b – M.D. Milshina; c – I.V. Pekov & A.V. Kasatkin.



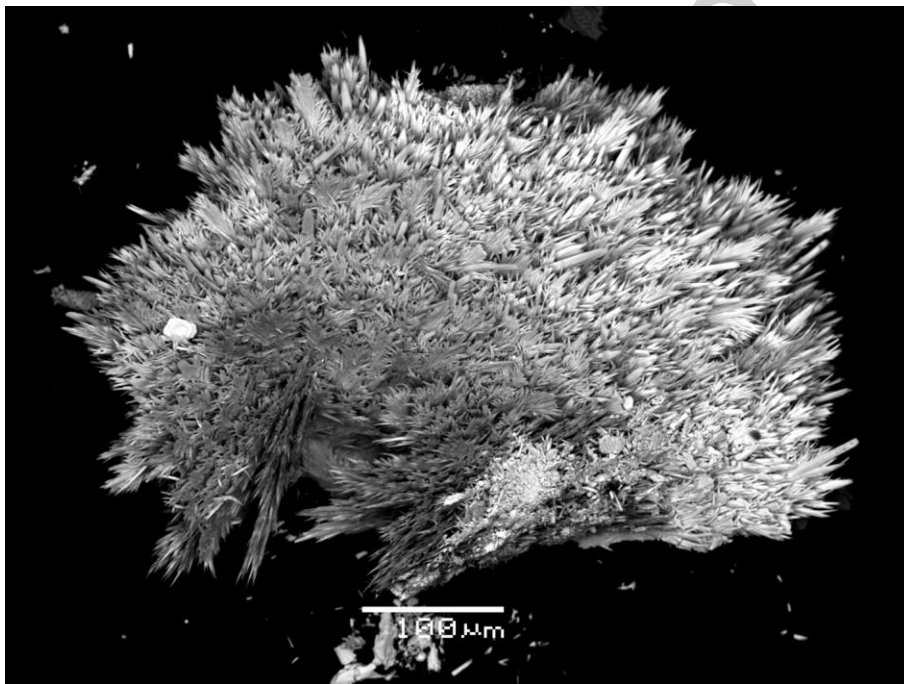
a



b



c



d

Figure 2. Ozernovskite crystals and aggregates: (a, b) sprays of prismatic ozernovskite crystals on dense clusters of split sonoraite crystals; (c) bush-like aggregates of acicular ozernovskite crystals on sonoraite crystal crust; (d) radial aggregate of divergent spear-like ozernovskite crystals. SEM images, SE mode. FOV width (mm): (a, c, d) 0.7; (b) 0.2.

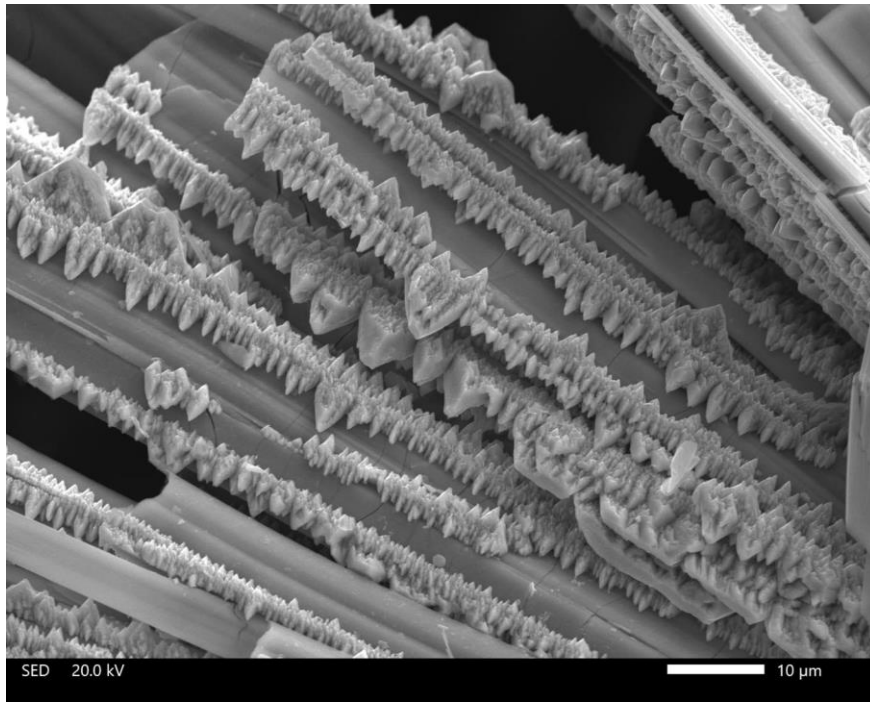


Figure 3. Parallel intergrowths of numerous lenticular crystals of emmonsite epitactically overgrowing long-prismatic ozernovskite crystals. SEM image, SE mode.

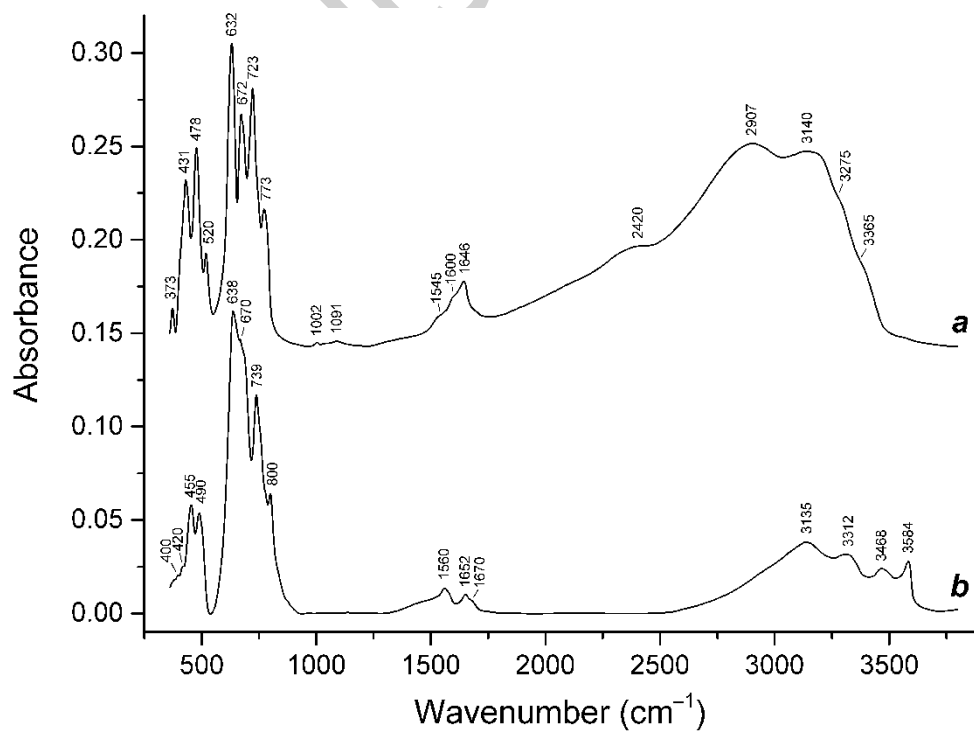


Figure 4. Powder infrared absorption spectra of (curve *a*) ozernovskite and (curve *b*) emmonsite, both from the Ozernovskoe deposit.

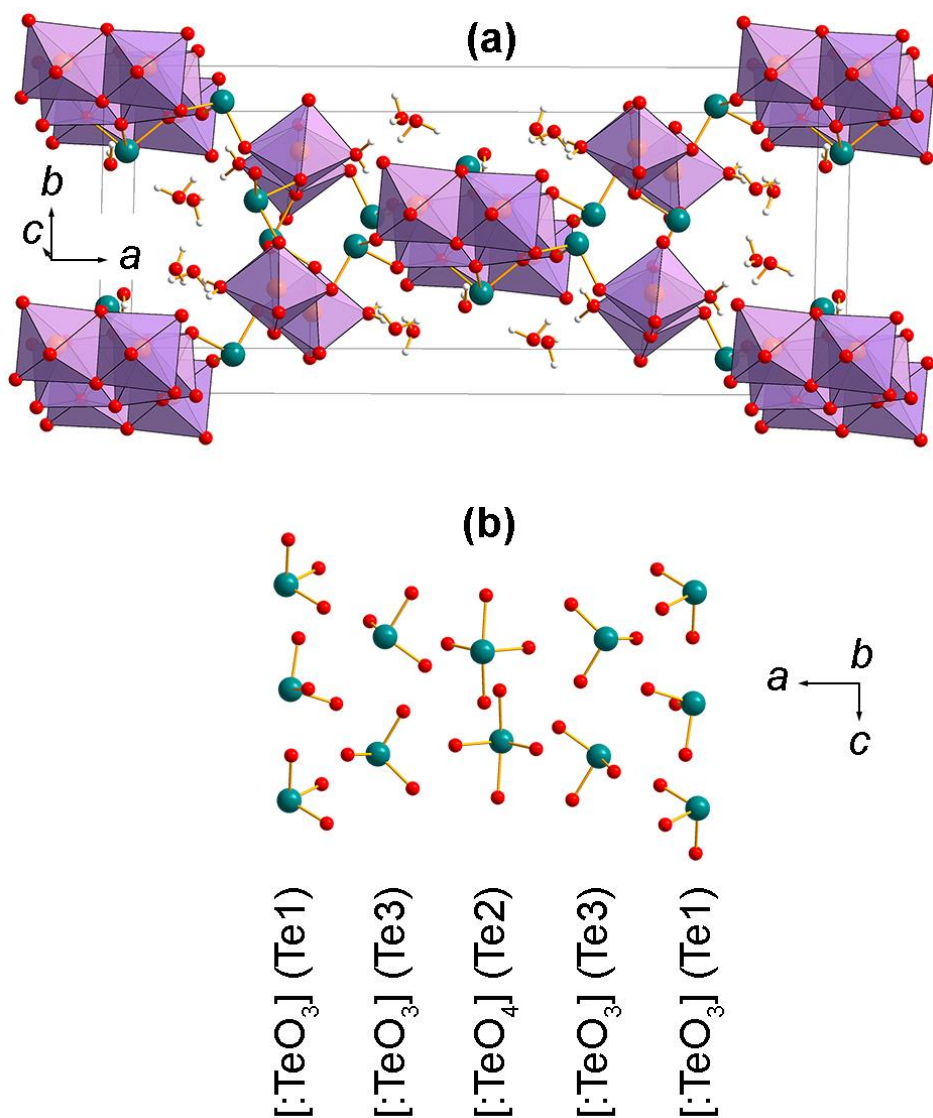


Figure 5. Crystal structure of ozernovskite. (a) An open framework composed of dimers of edge-sharing $[\text{FeO}_5(\text{H}_2\text{O})]$ octahedra and the similar dimers of $[\text{FeO}_6]$ octahedra, trigonal pyramids $[:\text{TeO}_3]$ and polyhedra $[:\text{TeO}_4]$ (the symbol ":" means lone electron pair belonging to Te^{4+}). Water molecules populate the channels propagating along the c axis. (b) Arrangement of the Te polyhedra in the structure. Legend: purple octahedra – FeO_6 ; grey-green balls – tellurium; red balls – oxygen; white balls – hydrogen.